Wood's anomalies and spectral uniformity of focusing diffractive optical elements

Hallvard Angelskår,[1,*] **Ib-Rune Johansen,**[2] **Matthieu Lacolle,**[2] **and Aasmund S. Sudbø**[3]

[1]*University of Oslo, Center for Materials Science and Nanotechnology, Department of Physics, PO Box 1048 Blindern, N-0316 Oslo, Norway*
[2]*SINTEF ICT, Microsystems and Nanotechnology, Gaustadalléen 23 C, N-0373 Oslo, Norway*
[3]*University of Oslo, Faculty of Mathematics and Natural Sciences, University Graduate Center, PO Box 70, N-2027 Kjeller, Norway*

*hallvard.angelskar@fys.uio.no

Abstract: We report on simulations and measurements of focusing diffractive optical elements, fabricated as two-level binary optics. The diffractive optical elements are designed to separate and focus four specific wavelengths in the infrared. The simulations are based on a local linear grating model, and predict anomalies similar to Wood's anomalies known from grating diffraction theory. The anomalies are also seen in the measurements, and are excited at the DOE locations predicted by the simulations. The given examples illustrate the usefulness of the model for evaluation of DOE designs. We also present a comparison of the response and spectral uniformity between two different versions of the four-wavelength diffractive optical elements. In the first version, the optical functions for all the four wavelengths are incorporated into the same surface pattern, covering the whole patterned area. In the second version the pattern for each wavelength is kept separate, and cover one fourth of the area, forming a mosaic of the four individual patterns.

© 2010 Optical Society of America

OCIS codes: (050.1380) Binary optics; (050.1970) Diffractive optics; (050.1965) Diffractive lenses.

References

1. R. F. Wolffenbuttel, "State-of-the-art in integrated optical microspectrometers," IEEE Trans. Instrum. Meas. **53**, 197–202 (2004).
2. O. Løvhaugen, I.-R. Johansen, K. A. H. Bakke, B. G. Fismen, and S. Nicolas, "Dedicated spectrometers based on diffractive optics: design, modelling and evaluation," J. Mod. Opt. **51**, 2203–2222 (2004).
3. H. Angelskår, I.-R. Johansen, M. Lacolle, H. Sagberg, and A. S. Sudbø, "Spectral uniformity of two- and four-level diffractive optical elements for spectroscopy," Opt. Express **17**, 10206–10222 (2009).
4. E. Noponen, J. Turunen, and A. Vasara, "Electromagnetic theory and design of diffractive-lens arrays," J. Opt. Soc. Am. A **10**, 434–443 (1993).
5. Y. Sheng, D. Feng, and S. Larochelle, "Analysis and synthesis of circular diffractive lens with local linear grating model and rigorous coupled-wave theory," J. Opt. Soc. Am. A **14**, 1562–1568 (1997).
6. A. Herbjørnrød, K. Schjølberg-Henriksen, H. Angelskår, and M. Lacolle, "Resist evaluation for fabrication of diffractive optical elements (DOE) with sub-micron resolution in a MEMS production line," J. Micromech. Microeng. **19**, 125022 (2009).
7. M. C. Hutley, Diffraction gratings, Techniques of Physics, London: Academic Press, (1982).
8. GD-Calc. http://software.kjinnovation.com/GD-Calc.html.

---

1. Introduction

Diffractive optical elements (DOEs) are useful components in small, lightweight and low-cost spectrometer systems. Several such systems have been realized, see for instance [1] for a review of integrated microspectrometers. In [2] and [3] a DOE was described which acts as a focusing, beam splitting and dispersive element in a spectroscopy application. The task of the spectrometer is to characterize different polymer materials by studying the absorption of several different wavelengths in the infrared. The sample is illuminated with white light, and the transmission is imaged onto the DOE. The task of the DOE is then to focus light of the specific wavelengths into different directions. The spectrum of the diffracted light is dispersed within each focal line. The foci for the different wavelengths are then scanned across a detector, such that the correct wavelengths are detected. Fig. 1 shows a sketch of the DOE system principle.
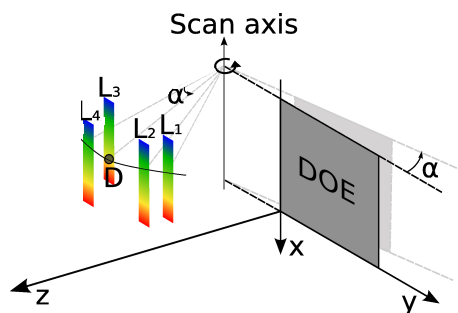

Fig. 1. After light is transmitted through a sample, the DOE is used to focus the light into four focal lines (L1-L4). Each focal line contains a spectrum in the near infrared. When the DOE is rotated the spectra are scanned across the detector. Four wavelength bands centered on the design wavelengths are sequentially detected.

The surface profile of the diffractive optical elements consists of grooves similar to a diffraction grating, but in a more complex pattern. The groove profiles can be realized in several different ways. Using silicon fabrication technology, a multilevel approximation is common, in which an ideal continuous profile is approximated by two or more levels, or steps, with vertical walls. These levels can be etched in silicon by standard reactive ion etching techniques.

We showed in [3] that the DOEs designed with four levels have a much better spectral uniformity than the corresponding DOEs with two levels. A better spectral uniformity means that the quality of the spectroscopic measurement is much less dependent on the uniformity of the illumination of the element. Thus, for this particular application and design, the four-level DOE was preferred. However, there are advantages and disadvantages with both the two- and four-level DOEs. The two-level DOE yields a lower diffraction efficiency, and also the effect of Wood's anomalies are much stronger than for the four-level DOE, as shown in [3]. On the other hand, the fabrication of four-level DOEs is more demanding since it requires the realization of smaller linewidths, and also two photolithography steps with the alignment of a second mask to the pattern realized by the first mask. In some cases it can be advantageous to fabricate the DOE in a MEMS production line, for instance for integration in micro-opto-electromechanical systems (MOEMS). Very small line-widths and precise mask alignment can be challenging in some MEMS production lines. Thus, there is a limit where the fabrication of four-level DOEs is not feasible, and the two-level DOE is the only practical choice. Furthermore, the appearance of Wood's anomalies is dependent on the geometry of the system, and the design wavelengths. Thus, for a given set of design wavelengths, the system geometry can in principle be designed such that the Wood's anomalies are avoided. In light of this, the simulation method presented

in [3] is a valuable tool to test a given design before fabrication.

In [3] the main reason for the large variations in spectral uniformity for the two-level DOE was attributed to the Wood's anomalies. The excitation of the anomalies depends amongst other parameters on the incidence angle and the groove width on the DOE. Thus, the excitation can be associated with certain positions on the DOE, when the geometry of the setup is known. In [3] these positions were predicted in simulations, using the local linear grating model [4, 5]. However, the measurements of the two-level DOE in [3] did not clearly exhibit the location of one of the two predicted anomalies. It was proposed that the reason this anomaly was not sharply localized could be due to two effects not included in the model. These effects were the significant roughness of the grooves in that particular two-level DOE, and the mixing of the surface patterns for different wavelengths in the multi-wavelength (mélange) DOE. In this paper we return to the two-level DOE, and report on measurements carried out on a new set of DOEs fabricated at SINTEF ICT. The fabrication of this new set of DOEs was recently presented in [6]. The DOEs were realized with smooth groove walls, as opposed to the two-level DOEs of [3] where the walls were rough. Thus, the groove profiles of the new DOEs more closely resemble those of the model. The simulations predict the excitation of Wood's anomalies of both the Rayleigh and resonance type, known from standard grating diffraction theory [7]. We show in this paper that both anomalies also appear in the measurements when the DOEs are fabricated with smooth groove walls. This further increases the usefulness of the local linear grating model used in [3] and the present paper, and shows that resonance anomalies can indeed be excited for ideally fabricated multi-wavelength focusing DOEs.

In Section 2, we briefly present the fabricated DOEs and the measurement setup. In Section 3, we outline the simulation method which is the same as in [3]. In Section 4 we compare the measurements with simulations for mélange DOEs, which are multi-wavelength DOEs where the optical functions for all four wavelengths are incorporated into the same surface pattern (as explained further in the next section). In Section 4.2 we compare specifically the spectral uniformity of four-wavelength mélange DOEs with that of the corresponding mosaic DOEs, where the patterns for each wavelength are kept separate and each cover one fourth of the patterned surface.

2. DOE test structures and measurement setup

The simplest way to design a four-wavelength DOE such as described in the introduction, is to use four off-axis reflective Fresnel lens-like segments. Such a DOE is divided into separate patterns corresponding to the four wavelengths. Each pattern is then covering one fourth of the total patterned surface. We call this type of DOE a mosaic DOE. Each separate diffractive lens pattern is then designed to focus a certain wavelength onto the detector, for a certain DOE orientation. By a simple rotation of the DOE, one can sequentially focus each wavelength onto the detector.

In a practical application the illumination of the DOE may be non-uniform. In this case it is advantageous to include the optical functions for all the design wavelengths in the same surface area. Thus there is a single pattern working for each of the wavelengths simultaneously, covering the whole surface area. We call this solution a mélange DOE. Again, a rotation of the DOE is used to switch between the different wavelengths. The design of such mélange DOEs was described in [2] and [3]. Filtering light into four spatially separated foci naturally comes at the cost of optical power, as the incident light is always diffracted into the four different directions, while only one is directed towards the detector. Both mélange and mosaic DOEs were fabricated. The mosaic and mélange DOEs were realized with a groove depth of $\lambda_{avg}/4$, where λ_{avg} is the mean of the four design wavelengths, as given in Fig. 3. In Section 4.2, we compare the response from the mélange DOEs to that of the mosaic DOEs.
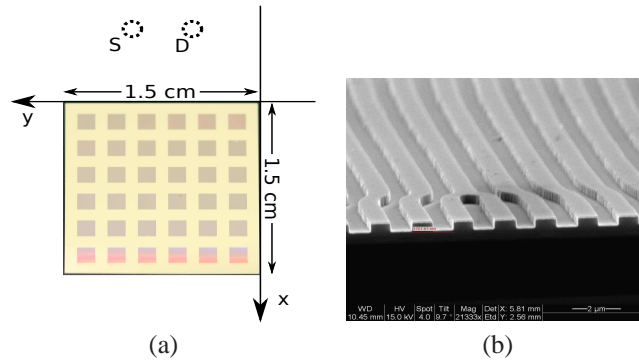
Fig. 2. a) The gold coated silicon DOE with 6x6 patterned squares. The circles above the DOE indicate the position of the source S and detector D projected into the DOE plane. b) An SEM image showing a cross-section of the two-level mélange DOE for four wavelengths. The groove width in the cross section in this image is approximately 875 nm. The bifurcation, or split ridge, is due to the "mixing" of patterns for four wavelengths.

A photograph of a mélange DOE is given in Fig. 2(a), and in 2(b) we present an SEM image of a small part of the surface pattern of a mélange DOE. The DOEs were patterned in 6x6 squares with a pitch of 2.5mm, each with sides of 1.5mm, see Fig. 2(a). For the mosaic DOEs, each such square was divided into four sections with different patterns for the four different wavelengths. The total size of the DOE is 1.5 cm by 1.5 cm. The piecewise patterning reduces the amount of data needed to describe the surface pattern, compared to a continuous surface patterning. Also, during measurements a screen with a small aperture is placed in front of the DOE to measure the local response at specific locations. The piecewise patterning allows for simple and precise navigation of this aperture.

The presented DOEs are test structures not designed for applications. A DOE used for spectroscopy applications would naturally be continuously patterned to take advantage of all the incident optical power. The fabrication of the test DOEs was described in [6], with an emphasis on the photolithography process developed to achieve DOEs with vertical walls within a MEMS processing line. All the DOEs were fabricated in silicon, and sputtered to achieve an approximately 60 nm thick gold layer.

As mentioned, a movable screen with a small aperture is moved in front of the DOE in order to study the local response from the 6x6 different positions on the DOE. The DOE is illuminated by white light through an optical fiber, and the filtered wavelengths are detected by an infrared detector. The geometry of the measurement setup is described in detail in [3]. Each measurement was performed twice, once with the aperture open, and once with the aperture closed to determine the background signal. The background signal was then subtracted from the raw measurement data in order to remove the effect of detected stray light from the setup.

3. Simulations

The simulations are based on a local linear grating model [4,5], in which small parts of the DOE surface are approximated by ideal diffraction gratings. For a given position, the corresponding ideal diffraction grating is determined as described in [3]. The diffraction problem for this grating is then solved with the rigorous coupled-wave method implemented in the GD-Calc program [8]. The result of the simulation is given as diffraction efficiency distributed on the propagating diffraction orders. The grating of the approximation model is designed such that the diffraction angle of the $m = -1$ diffraction order equals the angle between the DOE and the

detector at the specific position, disregarding conical diffraction.

In order to take into account the finite size of the measurement aperture, simulations were carried out for many points within each aperture. Thus the final simulation results were obtained by averaging over simulations where the incidence and diffraction angles of the model were computed for 7x7 different points, selected with a pitch of 0.2 mm within the aperture used in the measurement. The simulated diffraction efficiency variation within the aperture is typically much less than 1% for most x- and y-positions on the DOE, but can be as large as approximately 30% for the anomalous regions. The same general trends are seen for simulation results sampling different points within each aperture. However, since the whole aperture is illuminated during the measurements, a sampling of the whole aperture in the simulations yields a better representation than selecting a single point within each aperture.

4. Results

We report on three main findings from the simulations and measurements. First, the DOE positions which yields the Wood's anomalies are precisely predicted by the simulations, as verified in the measurements. Second, Wood's anomalies are seen to dominate the spectral uniformity of the DOEs. Third, the mosaic DOE is seen to yield poorer spectral uniformity than the mélange DOE, making the latter a very attractive choice for the multi-wavelength DOE.

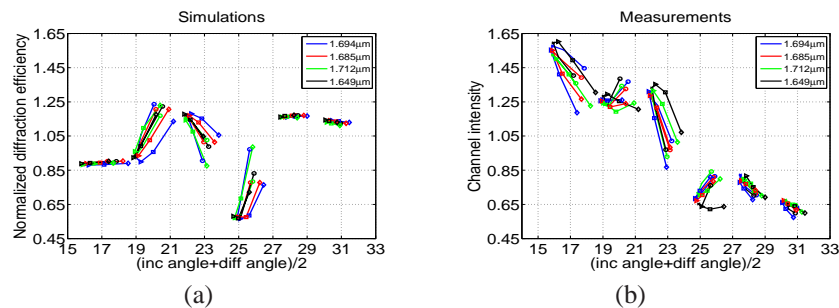### 4.1. Comparison between simulations and measurements

Fig. 3. Comparison of the DOE response in a) simulations and b) measurements. Data points for a given x-coordinate are connected with a line. In total there are six clusters of data points, each consisting of four sets of connected points corresponding to the four wavelengths, as given by the color coding. There is one such cluster for measurements done at each of the six x-positions on the DOE. For example, the points around $31°$ in a) correspond to $x = 6$ and $y = 1...6$ for the four wavelengths. The diffraction efficiency and intensity is plotted against the mean of the diffraction and incidence angles for each given position. a) Diffraction efficiency from simulations. The diffraction efficiency is normalized to the average efficiency for each wavelength, and averaged over simulation results for 7x7 different points within the aperture for each aperture position. b) Detector intensity normalized to the average intensity for each wavelength.

The simulations yield diffraction efficiency distributed on the propagating orders. We plot the diffraction efficiency for the -1st order which is directed towards the detector position. The diffraction efficiency can not directly be compared to the detected intensity of the measurement, as will be discussed later. However, for our purpose we see that the intensity shares some features with the diffraction efficiency. In Fig. 3(a) simulation results are given, and Fig. 3(b) shows the measurement results. In both cases the response for each wavelength is normalized to the average response of that wavelength for all DOE positions. Each data point in the figures
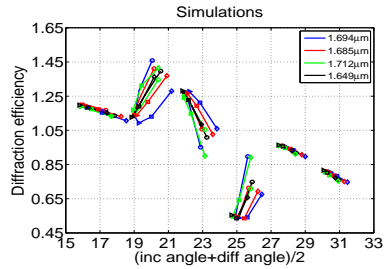
Fig. 4. Diffraction efficiency as in Fig. 3(a), but corrected with a normalized distance factor $1/r^2$ where r is the normalized distance from the source to a given DOE position. The correction factor is introduced in order to take into account the fact that the illumination is varying across the DOE.

corresponds to the normalized peak intensity (for measurements) or diffraction efficiency (for simulations) for a wavelength as given by the color coding. For each x-position on the DOE (see Fig. 2), the 6 y-positions are connected with a solid line. The source and detector are positioned above the DOE at the same value of the coordinate x, see Fig 2(a). Thus the variations in incidence and diffraction angle are largest in the x-direction. Due to the rotation of the DOE, the angles are not symmetrically distributed over the 6 y-positions for all the wavelengths. In the figures we plot the diffraction efficiency and intensity against the mean of the incidence and diffraction angles at each position.

In Fig. 3 we see that there is a peak at around $21°$, and a minimum near $25°$ in the results from both the simulations and measurements. As discussed in [3], the +1st diffraction order will be pointing into the surface at around 18-$20°$ incidence. When one diffraction order goes from propagating to evanescent, the energy is redistributed into the remaining propagating orders. The changes in the number of propagating orders lead to the rapid variations, i.e. Rayleigh anomaly, seen around $21°$ in Fig. 3 (in the figure the response is plotted for the average of the incidence and diffraction angles). The dip in the response with a minimum near $25°$ is due to a resonance type Wood's anomaly. Both of these anomalies were predicted in simulations, and discussed in detail in [3]. However, the measurements reported in [3] did not show a localized resonance anomaly, but this is seen here in Fig. 3(b).

In Fig. 3(b), we see that the measured intensity is generally lower for higher incidence angles (and diffraction angles). This is partly due to the fact that the corresponding positions (high x-positions) are further away from the source. If we for simplicity assume a simple $1/r$ dependence of the amplitude of the illumination, as for a spherical wave, we can introduce a correction factor ($1/r^2$) for the simulation results. The result of this is shown in Fig. 4. The result of including such a correction factor is shown in Fig. 4. A further correction would be needed to describe the refocusing of light from the DOE on a finite-area detector, but even with this deficiency in modeling, Fig. 4 agrees well with the measurements in Fig. 3(b).

4.2. Spectral uniformity of mélange and mosaic DOEs

In order to study the spectral uniformity of the DOEs, we use the same normalization procedure as in [3]. For all the wavelengths, at each DOE position the response is first normalized to the average response of the same wavelength over all DOE positions. Then it is normalized to the average response of all the wavelengths at the current position. Thus the value of the points in Fig. 5 essentially amounts to a factor describing how much the peak intensity of one wavelength band deviates from the average peak intensity of all the wavelength bands at that DOE position.

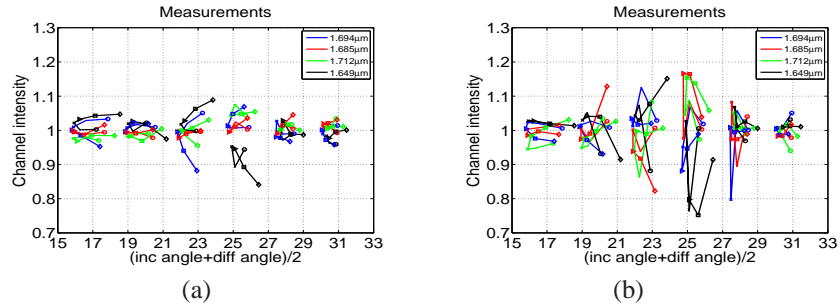Referring to Fig. 5, the spectral uniformity for the mosaic DOE in Fig. 5(b) was found to be

Fig. 5. Comparison of the normalized DOE response in measurements. a) shows normalized intensity for the mélange DOE, and b) shows normalized intensity for the mosaic DOE. Data points for a given *x*-coordinate are connected with a line. In total there are six clusters of points, corresponding to six *x*-positions. Each cluster consists of four sets of connected points corresponding to the four wavelengths, as given by the color coding.

worse than for the mélange DOE in Fig. 5(a). We also see that the largest variations coincide with the resonance anomaly around 25°. One reason for the difference in spectral uniformity can be that the mélange DOE pattern is a combination of the pattern for four wavelengths. Thus the sharply localized anomalies will not be as dominant as in the design where the pattern for each wavelength is kept separate. This hypothesis is also supported by the fact that the anomalies are typically stronger (than in the mélange DOE measurements) in the simulations, see Fig. 6, which are based on single diffraction gratings that more closely resemble the single-wavelength patterns of the mosaic DOE.
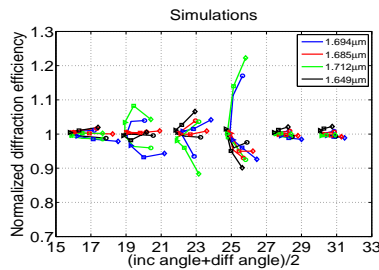

Fig. 6. Normalized DOE response showing the spectral uniformity from simulations. We see that the resonance anomaly around 25° degrees is stronger than in the measurements on the mélange DOE in Fig. 5(a), but similar in strength with that of the mosaic DOE 5(b).

5.   Conclusions

We have measured the spectral response of two-level diffractive optical elements (DOEs) that have been fabricated in silicon and coated with gold. The measured response was compared with simulations based on a local linear grating model. Both Rayleigh and resonance type Wood's anomalies affect the response, both for mosaic and mélange type multi-wavelength DOEs.

The Wood's anomalies in focusing diffractive optical elements were previously discussed in [3], but only the Rayleigh type anomaly was found to be clearly localized in the measurements. It was proposed that this could be due to the roughness of the groove walls in the two-level surface patterns mélange DOE studied in that paper, or due to the mixing of patterns in mélange

DOEs. In the present paper, new two-level DOEs were presented, where the surface pattern was successfully realized such that the groove walls were smooth. The measurements clearly show both anomalies in the response of the DOEs. Thus we find that localized Wood's anomalies of both the Rayleigh and resonance type are indeed observed for mélange DOEs when the groove walls are smooth. For the present application the anomalies lead to a poor spectral uniformity, and a four-level DOE design as discussed in [3] is preferable. However, the present results show that the local linear grating model is very valuable for prediction of the locations of the Wood's anomalies. Thus, the simulations may in some cases be used to find a two-level DOE design where the anomalies are not excited, which may allow for a better spectral uniformity.

Additionally, the spectral uniformity is seen to be worse for the mosaic DOEs than for the corresponding mélange DOEs. Thus the patterning of a single surface for all the design wavelengths is beneficial for the spectral uniformity.